



Full Length Article



Yanang water extract exhibits a protective effect against methomyl-induced cytotoxicity in RAW 264.7 cells via suppression of apoptosis and cell cycle arrest

Boonyarit Kukaew^{a,b,1}, Wanna Sirisangtragul^{a,1}, Sittiruk Roytrakul^c, Anupong Joompang^d, Napaporn Roamcharern^b, Anupong Tankrathok^{b,e}, Patralak Songserm^b, Sakda Daduang^{b,f}, Sompong Klaynongsruang^{b,g}, Nisachon Jangpromma^{b,g,*}

^a Department of Integrated Science, Forensic Science Program, Faculty of Science, Khon Kaen University, Khon Kaen 40002, Thailand

^b Protein and Proteomics Research Center for Commercial and Industrial Purposes (ProCCI), Faculty of Science, Khon Kaen University, Khon Kaen 40002, Thailand

^c Functional Proteomics Technology Laboratory, National Center for Genetic Engineering and Biotechnology, National Science and Technology Development Agency, Pathumthani 12120, Thailand

^d Faculty of Pharmaceutical Sciences, Burapha University, Chon Buri 20131, Thailand

^e Department of Biotechnology, Faculty of Agricultural Technology, Kalasin University, Kalasin 46000, Thailand

^f Department of Pharmacognosy and Toxicology, Faculty of Pharmaceutical Sciences, Khon Kaen University, Khon Kaen 40002, Thailand

^g Department of Biochemistry, Faculty of Science, Khon Kaen University, Khon Kaen 40002, Thailand

ARTICLE INFO

Keywords:

Apoptosis
Bioactive compound
Cell cycle
Cytotoxicity
Insecticide
Tiliacora triandra

ABSTRACT

Methomyl, an extremely hazardous substance, is widely used for controlling insects and pests in agricultural production. This compound can cause several illnesses in humans. In this research, we determined the alleviation potential of Yanang water extract (YWE) against methomyl-induced cytotoxicity in RAW 264.7 macrophage cells and examined the underlying mechanisms of action. The YWE (2.5 – 10 µg/mL) exhibited no toxicity against RAW 264.7 cells, whereas methomyl significantly reduced RAW 264.7 cell growth, resulting in the progression of apoptosis and cell cycle arrest. Supplementation of YWE on methomyl treated RAW 264.7 cells revealed a pronounced protective effect via the suppression of caspase-9 and caspase-3 mRNA expression levels. Proteomics studies were used to assess the effect of methomyl on RAW 264.7 cells, revealing an increase of proteins associated with apoptosis and cell cycle arrest, whereas in the YWE co-treatment condition these proteins were suppressed. Moreover, an increase in proteins involved with cell cycle progression and anti-apoptosis was found in YWE co-treatment. Our findings suggest that YWE is potentially involved in mitigating methomyl-induced cytotoxicity, via the suppression of apoptosis and cell cycle arrest.

1. Introduction

Pesticides such as herbicides, insecticides, fungicides and rodenticides have been widely used in recent years to enhance agricultural yields in many countries. Although contributing to agricultural output improvement, pesticide contamination has negative impacts on human health and causes environmental imbalances (Tudi et al., 2021). Among the pesticides, insecticides are currently ranked as the top three pesticides used in Thailand, with a proportion of imports in the year 2021 of 10,294.3 metric tons (Sapbamrer et al., 2023).

Methomyl, a commonly used carbamate insecticide, is raising concerns due to its frequent detection in food and the environment, despite being less toxic than older alternatives (Trachantong et al., 2017). It induces acute cholinergic poisoning in mammals by inhibiting acetylcholinesterase, leading to the accumulation of acetylcholine and damage to the nervous system (Trachantong et al., 2017). Methomyl exposure triggers cellular damage (DNA, proteins, lipids) through reactive oxygen species (ROS)-induced oxidative stress and may activate MAPK pathways, leading to apoptosis or necrosis (Heikal et al., 2014; He et al., 2022). Studies highlight its significant oxidative stress in mammals

Peer review under responsibility of King Saud University

* Corresponding author at: Department of Biochemistry, Faculty of Science, Khon Kaen University, Khon Kaen 40002, Thailand.

E-mail address: nisaja@kku.ac.th (N. Jangpromma).

¹ Equal contributions.

<https://doi.org/10.1016/j.jksus.2024.103229>

Received 14 November 2023; Received in revised form 26 April 2024; Accepted 26 April 2024

Available online 27 April 2024

1018-3647/© 2024 The Authors. Published by Elsevier B.V. on behalf of King Saud University. This is an open access article under the CC BY-NC-ND license (<http://creativecommons.org/licenses/by-nc-nd/4.0/>).

(Djefal et al., 2015). This necessitates the exploration of natural compounds to mitigate methomyl toxicity on immune cells.

Tiliacora triandra (Colebr.) Diels or Yanang is one medicinal plant that has been described for its detoxification ability in the human body and which might show the benefit of protecting against methomyl toxicity. Yanang belongs to the family of Menipermaceae and is an endemic plant of Southeast Asia (Singthong et al., 2009). In northeast Thailand, its leaf water extract is traditionally used in cooking to reduce bamboo shoot toxicity (Phunchago et al., 2015). Several studies have reported that Yanang leaf extract contains high levels of essential bioactive compounds including tannin, triterpene, saponin, phytol, α -tocopherol, flavonoids, phenolic compounds and minerals (Singthong et al., 2009; Phunchago et al., 2015; Thong-Asa et al., 2017). These bioactive compounds offer medicinal properties such as anti-fever, antibacterial, antimalarial, anticancer, anti-inflammation, antioxidant, and neuroprotective effects (Singthong et al., 2014; Thong-Asa et al., 2017). However, there is no research on the preventive effect of Yanang leaf extracts on methomyl-induced cytotoxicity in immune cell lines. Macrophages are one part of the innate immune response, having an important role in antigen presenting and the engulfing of antigens by phagocytosis (Nazimek et al., 2013). Accordingly, the roles of macrophages are in immune response initiation to regulate immunological function and are susceptible targets for chemical oxidants (Jang et al., 2015). Hence, macrophages may represent useful targets for developing new natural compounds to reduce toxicity from methomyl.

Therefore, this research aims to assess the protective effects of Yanang leaf extracts against methomyl-induced toxicity in RAW 264.7 murine macrophage cells. Various parameters were assessed, encompassing the percentage of cell cytotoxicity, apoptosis rate, and cell cycle arrest. Furthermore, alterations in mRNA expressions of apoptosis-related genes and proteomics profiling were examined to illuminate the mechanisms underlying the protective effects of Yanang leaf.

2. Materials and methods

2.1. Preparation of Yanang extract

The leaves of Yanang (*Tiliacora triandra*) were gathered from Khon Kaen province in the Northeastern region of Thailand. The leaves were washed under a tap, cut into small pieces, and ground with distilled water at a 1:8% w/v ratio. The extract was then filtered through cotton cloth. The filtrate was centrifuged at 6,068 \times g at 4 °C for 30 min. The pellet was discarded, and the supernatant was collected as Yanang water extract (YWE). The protein concentration and total phenolic content (TPC) were measured. The extract was kept cold (-20 °C) until further use in subsequent experiments.

2.2. Protein concentration measurement

The Bradford assay was employed to assess the concentration of protein (Bradford, 1976). Briefly, 1,000 μ L of Bradford dye was mixed with 1 μ L of YWE and incubated for 10 min. The absorbance was recorded at 595 nm (Microplate reader, Varioskan LUX, USA). The concentration of protein was subsequently determined using the BSA standard curve.

2.3. Total phenolic content (TPC) measurement

The TPC of YWE was assessed using the Folin-Ciocalteu (FC) reagent (Singthong et al., 2014). Briefly, 1,000 μ L of YWE was mixed with 100 μ L of FC reagent, 300 μ L of 20 % sodium carbonate, and 500 μ L of distilled water. The reaction mixture was incubated for 2 h at 50 °C, and a microplate reader (Varioskan LUX, USA) was used to record the absorbance at 765 nm. A calibration curve of standard gallic acid was used to convert the measured absorbance values into gallic acid equivalents (μ g GAE/mL), which served as a measure of the total phenolic

content.

2.4. Cell viability / cytotoxicity assay

RAW 264.7 cell viability (ATCC, Manassas, VA, USA) was evaluated using the MTT assay. In a 96-well plate, the cells (2.5×10^4 cells/well) were cultured for 24 h at 37 °C with 5 % CO₂ in DMEM (Dulbecco's Modified Eagle Medium). Afterward, cells were exposed to YWE for an additional 24 h at doses ranging from 2.5 – 10 μ g/mL. To assess the protective effect of YWE against methomyl-induced cytotoxicity in RAW 264.7, the cells were co-treated with 11,000 μ M methomyl and 2.5 – 10 μ g/mL of YWE for 24 h. Subsequently, the medium was substituted with 100 μ L of MTT solution (0.5 mg/mL) and incubated for 30 min at 37 °C with 5 % CO₂. The purple crystal (formazan) was then solubilized in 100 μ L of DMSO, and the absorbance at 570 nm was quantified using a microplate reader (Varioskan LUX, USA). To calculate cell viability (%), the following formula was used:

$$\% \text{ Cell viability} = (A570_{\text{test}}/A570_{\text{control}}) \times 100$$

where A570_{test} refers to the absorbance of cells treated with either YWE, methomyl, or co-treatment at 570 nm. A570_{control} refers to the absorbance of untreated cells at 570 nm.

2.5. Dual fluorescent staining apoptosis assay

Apoptosis was studied using the dual staining approach with acridine orange/ethidium bromide (AO/EB). RAW 264.7 cells (1.0×10^5 cells/well) were plated into a 48-well plate and cultured for 24 h at 37 °C with 5 % CO₂. After that, cells were incubated with 11,000 μ M methomyl and supplemented with YWE (2.5 – 10 μ g/mL) for an additional 24 h. After trypsinization, cells were resuspended in a fresh medium and centrifuged at 95 \times g for 5 min. Following this, a dual staining solution consisting of 10 mg/mL AO and 10 mg/mL EB in PBS was applied to stain the cell pellet in a 1:1 ratio. The cells were incubated in the dark for 15 min. A 10 μ L aliquot of the stained cell suspension was transferred to microscope slides, coverslipped, and observed under a fluorescence microscope (Carl Zeiss Microscopy, USA) for analysis of apoptotic morphology.

2.6. Flow cytometry-based apoptosis assay

After being plated into a 12-well plate, RAW 264.7 cells (1.5×10^5 cells/well) were cultured for 24 h at 37 °C with 5 % CO₂. After that, cells were exposed to 11,000 μ M methomyl and supplemented with YWE (2.5 – 10 μ g/mL) for 24 h. The cells were then trypsinized, suspended in fresh DMEM, and centrifuged at 95 \times g for 5 min. After rinsing the cell pellet with ice-cold PBS, cells were re-suspended in an appropriate volume of $1 \times$ Annexin V binding buffer (BioLegend, USA) to achieve 1×10^6 cells/mL. Annexin V-FITC (5 μ L) and propidium iodide (PI) (10 μ L) (BioLegend, USA) were then added to 100 μ L of this cell suspension. 400 μ L of binding buffer was added after the mixture was left in the dark for 15 min. Apoptosis rates were analyzed using a flow cytometer (BD FACS-Canto II, BD Biosciences, USA) with BD Accuri C6 software for data interpretation.

2.7. Flow cytometry-based cycle arrest assay

The cell cycle stage was assessed using PI staining. After treatment of RAW 264.7 cells with 11,000 μ M methomyl and various concentrations of YWE, as described earlier, cell pellets were collected, rinsed with ice-cold PBS, and fixed with 400 μ L of ice-cold 70 % ethanol at 4 °C overnight. The cells were then centrifuged at 95 \times g for 5 min and re-suspended in 200 μ L of PBS. 100 μ L of cell suspension was transferred into a flow tube and incubated in the dark with 2.5 μ L of RNase A (20 mg/mL) and 2 μ L of PI (1 mg/mL) for 30 min. After that, 400 μ L of PBS

was added to the cell suspension, and a Flow Cytometer (BD FACSCanto II, BD Biosciences, USA) was employed to assess the cell cycle.

2.8. Gene expressions study using real-time PCR

After RAW 264.7 cells were cultured and treated with 11,000 μM methomyl along with various concentrations of YWE, as described earlier, the cell pellets were harvested and processed for RNA extraction using Trizol reagent (Invitrogen, USA). The cDNA was synthesized according to the RevertAid First Strand cDNA Synthesis Kit (Thermo Fisher Scientific Inc, USA). The PCR mixture included 2 μL of cDNA, 10 μL of LightCycle® SYBR® Green I Master mix (Roche, Switzerland), and 1 μL of each primer (10 μM) in a total volume of 20 μL . All PCR reactions were amplified using the LightCycler 480 instrument (Roche, Switzerland). The annealing temperatures for each gene-specific primer were determined individually as listed in Table 1. The comparative $2^{-\Delta\Delta\text{CT}}$ approach was employed to determine the relative alterations in gene expression levels. The GAPDH gene was used to normalize target gene expression levels.

2.9. Proteomics analysis using liquid chromatography mass spectrometry

RAW 264.7 cells were cultured and treated with 11,000 μM methomyl and various concentrations of YWE as described earlier. Then, cells were harvested, and proteins were extracted using 50 mM Tris-HCl pH 7.0 and 0.5 % SDS, with sonication at amplitude levels of 80 % for 3 s. Centrifugation was performed at 9,481 $\times g$ for 15 min and the supernatant was used for protein extraction by incubating with ice-cold acetone containing 0.1 mM DTT (1:5 v/v ratios) for 16 h at -20°C . The protein was subsequently digested with trypsin at a ratio of 1:20 before being incubated at 37°C for 6 h. Peptides were fractionated by ultra-performance liquid chromatography (UPLC) and C_{18} -reverse phase chromatography. Quantitative data analysis was processed by Decyder Ms 2.0. Protein identification was conducted using Mascot. To visualize all possible intersections among proteome datasets, a Venn diagram was generated using the jvenn tool online.

2.10. Statistical methods

Data from three independent experiments are shown as means \pm SD. SPSS 20 software was used to conduct the statistical analysis. Duncan's multiple range test was employed for post-hoc comparisons after one-way ANOVA was used to evaluate differences between the treatment and control groups. A 0.05 threshold for statistical significance was applied.

3. Results

3.1. Protective effect of YWE against methomyl-induced cytotoxicity in RAW 264.7 cells

The YWE was analyzed for total protein and total phenolic content using the Bradford assay and the Folin-Ciocalteu method, respectively. The results indicate that YWE showed protein and total phenolic content at $7.42 \pm 0.24 \mu\text{g}/\text{mL}$ and $5.23 \pm 0.41 \mu\text{g GAE}/\text{mL}$, respectively. Rapid

protein concentration determination with the Bradford method was used for estimating YWE concentration in all experiments. MTT assay confirmed that YWE (2.5–10 $\mu\text{g}/\text{mL}$) exhibited no cytotoxicity in RAW 264.7 cells (99.08 – 100.78 % cell viability; Fig. 1A). These non-toxic YWE concentrations were then tested for protection against methomyl-induced cytotoxicity. In Fig. 1B, it is evident that methomyl at a concentration of 11,000 μM significantly induced cytotoxicity in RAW 264.7 cells, resulting in a viability of 48.16 %. However, co-treatment with YWE at concentrations of 2.5, 5, and 10 $\mu\text{g}/\text{mL}$ significantly reduced this effect, with cell viabilities of 57.13 %, 60.86 %, and

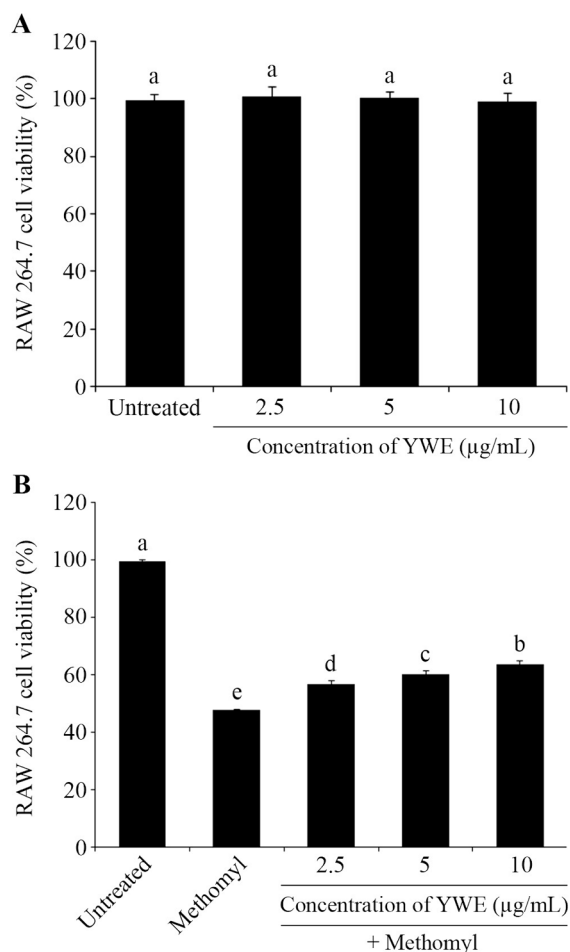


Fig. 1. Toxicity and protective effect of Yanang water extract (YWE) on methomyl-induced cytotoxicity in RAW 264.7 cells. (A) RAW 264.7 cells were exposed to YWE at concentrations of 2.5 – 10 $\mu\text{g}/\text{mL}$ for 24 h and then assessed using the MTT assay to determine their effect on cell viability. (B) The RAW 264.7 cells viability was measured using MTT assay after a 24 h incubation with 11,000 μM methomyl and supplementation with different concentrations of YWE (2.5 – 10 $\mu\text{g}/\text{mL}$) to evaluate its protective effect. The data are presented as mean \pm SD. Different letters on the top of each bar are significantly different, $p \leq 0.05$.

Table 1
Primer sequences for Real-time PCR.

Gene		Primer sequences (5' → 3')	Annealing ($^\circ\text{C}$)	Product size (bp)	Reference
Caspase-9	Forward	AGCCAGATGCTGTCCCATAC	55	124	AF262319
	Reverse	CAGGAGACAAAACCTGGGAA			
Caspase-3	Forward	CAGAGCTGGACTGCCGTATTGA	58	172	NM_012922
	Reverse	AGCATGGCGCAAAGTGACTG			
GAPDH	Forward	GAGAAACCTGCCAAGTATGATGAC	50	212	NM_008084.3
	Reverse	TAGCCGTATTCATTGTCATACCAG			

64.40 %, respectively (Fig. 1B).

3.2. Protective effect of YWE on methomyl-induced apoptosis in RAW 264.7 cells

The morphological apoptotic changes of RAW 264.7 cells with AO/EB dual staining are shown in Fig. 2A. AO stains live cells green, while EB stains apoptotic cells orange or red. The untreated control group showed predominantly green live cells, whereas the methomyl-treated group exhibited more apoptotic cells. Co-treatment with YWE (2.5 – 10 $\mu\text{g/mL}$) led to a concentration-dependent reduction in apoptotic cells.

Annexin V-FITC/PI flow cytometry confirmed methomyl-induced apoptosis in RAW 264.7 cells, which was significantly reduced with YWE treatment. Apoptotic cell percentages decreased in a concentration-dependent manner to 95.54 %, 71.26 %, and 57.87 % with 2.5, 5, and 10 $\mu\text{g/mL}$ of YWE, respectively (Fig. 2B).

Quantitative real-time PCR analysis revealed that methomyl treatment increased the expression of Caspase-9 and Caspase-3, key regulators of apoptosis, compared to the untreated group. Conversely, YWE co-treatment (2.5 – 10 $\mu\text{g/mL}$) downregulated these genes, suggesting that YWE may exert its protective effect against methomyl-induced apoptosis by regulating caspase expression (Fig. 2C, 2D).

3.3. Protective effects of YWE on cell cycle arrest induced by methomyl toward RAW 264.7 cells

DNA flow cytometric analysis indicated that methomyl significantly induced G_2/M cell cycle arrest by increasing the G_2/M phase from untreated control to 7.30 ± 0.28 . However, the percentages of RAW 264.7 cells in the G_2/M phase were significantly reduced by co-treatment with YWE (2.5, 5, and 10 $\mu\text{g/mL}$) to 6.45 ± 0.49 , 5.85 ± 0.30 , and 3.30 ± 0.18 , respectively. These findings suggest that YWE exerts protective effects by preventing methomyl-induced cell cycle arrest in RAW 264.7 cells, as evidenced by the reduced G_2/M phase population (Fig. 3).

3.4. Protective effects of YWE on the protein patterns in methomyl-induced toxicity in RAW 264.7 cells

The proteomic analysis revealed 681 proteins expressed in RAW 264.7 cells under 5 different conditions, including untreated control, methomyl alone, and co-treatment of methomyl with 2.5, 5, and 10 $\mu\text{g/mL}$ of YWE. The number of expressed proteins in each group was 550, 536, 575, 565, and 561, respectively (Fig. 4). A Venn diagram of differentially expressed proteins (DEPs) indicated that 423 proteins were shared commonly among all 5 conditions, while 7 proteins were only observed in the untreated control and methomyl treated groups, 5,

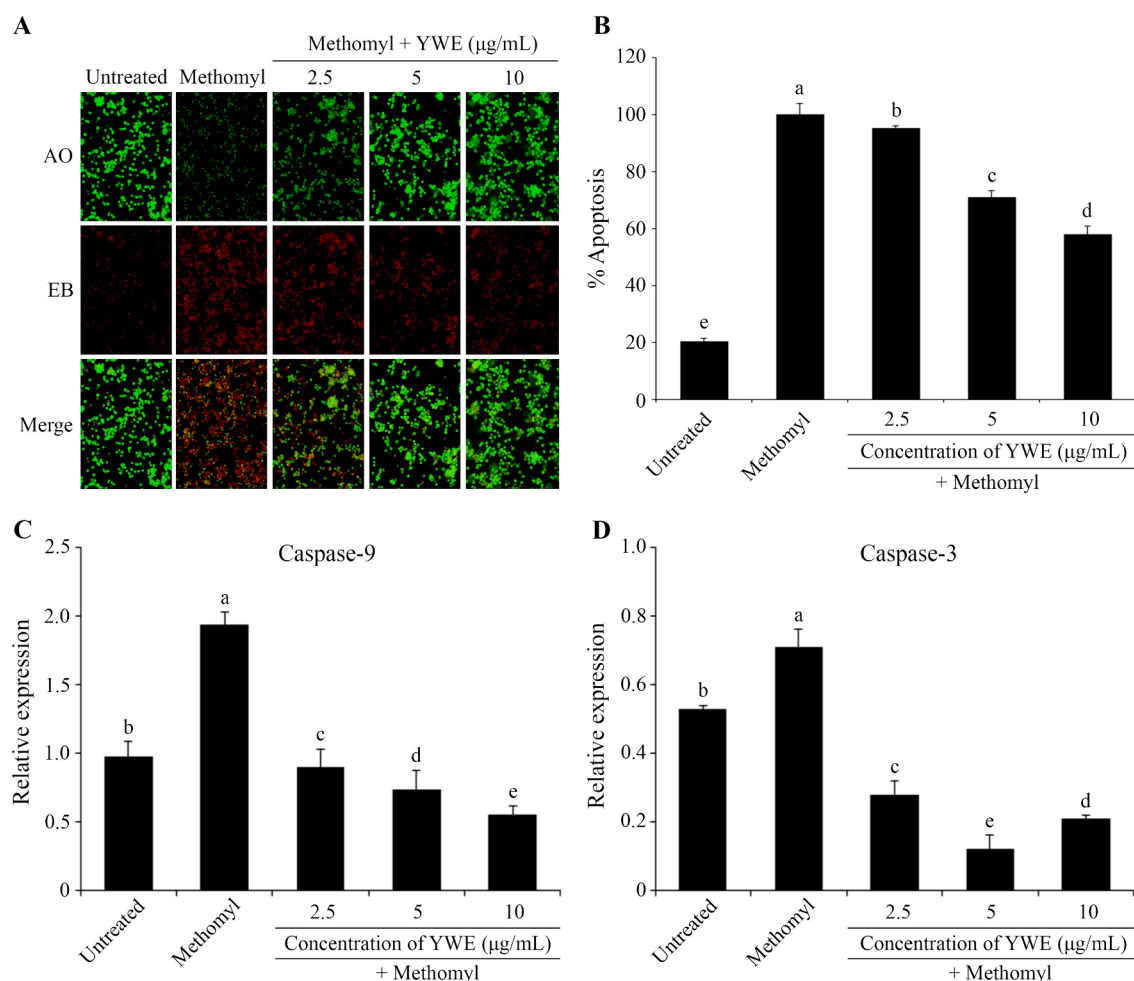


Fig. 2. Protective effects of Yanang water extract (YWE) on methomyl-induced apoptosis in RAW 264.7 cells. After treatment with methomyl and different concentrations of YWE (2.5 – 10 $\mu\text{g/mL}$) for 24 h, RAW 264.7 cells were stained with AO/EB and observed under fluorescence microscopy (20 \times) (A). The cells undergoing apoptosis were further measured by annexin V-FITC/PI flow cytometry assay and the apoptosis rate was determined and represented as a bar graph (B). The protective effect of YWE on apoptosis related genes, Caspase-9 (C) and Caspase-3 (D) was assessed through real-time PCR. The data are presented as mean \pm SD. Different letters on the top of each bar are significantly different, $p \leq 0.05$.

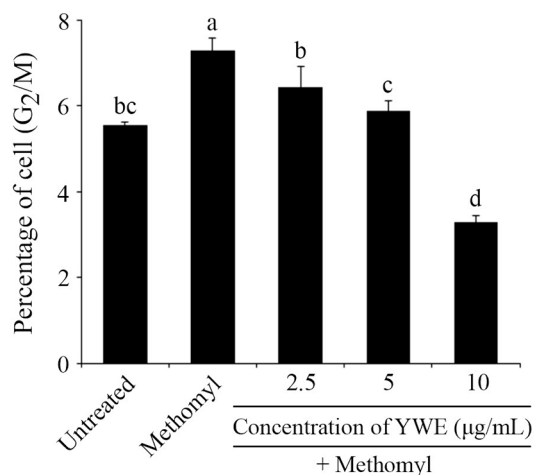


Fig. 3. Protective effect of Yanang water extract (YWE) on methomyl-induced cell cycle arrest in RAW 264.7 cells. After treatment with methomyl and different concentrations of YWE (2.5 – 10 µg/mL) for 24 h, RAW 264.7 cells were stained with PI and measured by flow cytometry. The percentage of RAW 264.7 cells in G₂/M peak is presented as mean ± SD. Different letters on the top of each bar are significantly different, $p \leq 0.05$.

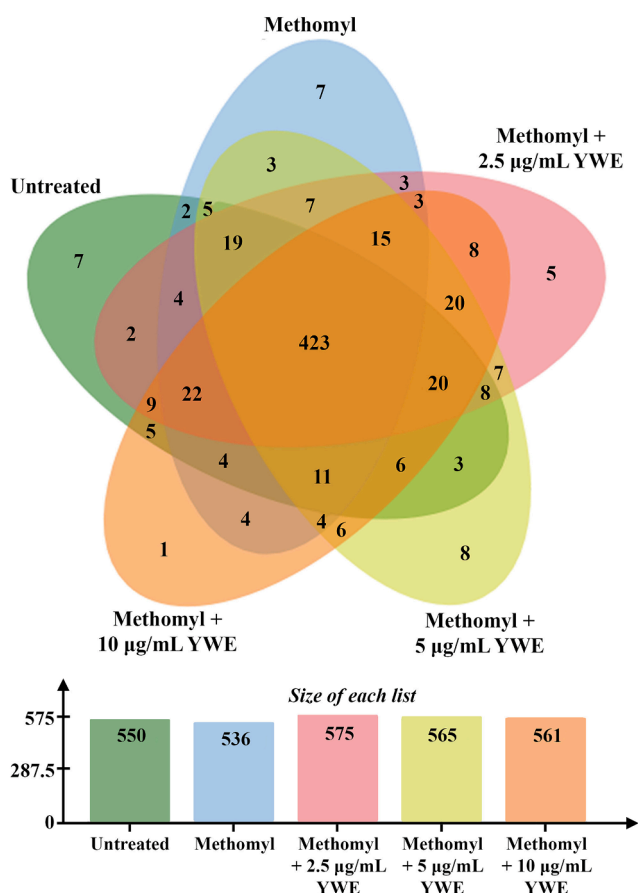


Fig. 4. Venn diagram presenting the expressed proteins of 5 treatments, including untreated control (550 proteins), methomyl treatment (536 proteins), and supplementation of 2.5 µg/mL Yanang water extract (YWE) (575 proteins), 5 µg/mL YWE (565 proteins), and 10 µg/mL YWE (561 proteins) to methomyl treated RAW 264.7 cells.

8 and 1 proteins were only observed in co-treatment of methomyl with 2.5, 5, and 10 µg/mL of YWE, respectively (Table S1). The functional proteins related to cell death and cell cycle pathway are indicated in Table 2-4. Table 2 lists the proteins exclusively observed in each group, which have known functions in apoptosis and cell cycle pathways. Of these, 4 proteins were only found in the methomyl treated group, including RAC-alpha serine/threonine-protein kinases (AKT1), Gamma-aminobutyric acid receptor subunit alpha-3 (GBRA3), LAG1 longevity assurance homolog 1 (LASS1) and programmed cell death protein 2-like (PDD2L). Meanwhile, co-treatment with 2.5 – 10 µg/mL of YWE altered functional proteins by promoting an expression of CUB and sushi domain-containing protein 1 (CSMD1) at a dose of 2.5 µg/mL,

Table 2

The list of functional proteins that noticeably appear only in each treatment.

Gene name	Matched protein	t-Test (p)	Function	Reference
Appears only in methomyl treated group				
AKT1	RAC-alpha serine/threonine-protein kinase	0.96	Relates to cell proliferation, apoptosis and survival	Hou et al., 2022
GBRA3	Gamma-aminobutyric acid receptor subunit alpha-3	0.91	Promotes apoptosis and differentiation in T-helper cell type-2	Meng et al., 2016
LASS1	LAG1 longevity assurance homolog 1	0.75	Inhibits proliferation, induces apoptosis in HepG2 HB cells through mitochondrial apoptotic, NF-κB and cell cycle signaling pathways (LASS2)	Yang et al., 2019
PDD2L	Programmed cell death protein 2-like	1.00	Related to ceramide synthesis which might promote cell cycle arrest and apoptosis (LASS5)	Xu et al., 2005; Gomez-Larrauri et al., 2020
			Deletes lymphocytes by reducing lymphocyte proliferation and cytokine production (PD-1)	Berntsson et al., 2018
			Promotes apoptosis, suppresses cell transformation by inhibiting protein translation (PDCD-4)	Lankat-Buttgereit and Goke, 2003
Appears only in co-treatment of methomyl and 2.5 µg/mL YWE group				
CSMD1	CUB and sushi domain-containing protein 1	0.64	Suppresses tumor progression	Blom, 2017
Appears only in co-treatment of methomyl and 5 µg/mL YWE group				
DLX6	Homeobox protein DLX-6	0.68	Anti-necrotic effects and promotes cell proliferation (DLX-2 and family)	Lee et al., 2011
SPTA1	Spectrin alpha chain, erythrocyte	0.62	Target of caspases	Karanam et al., 2010
TRIPC	E3 ubiquitin-protein ligase TRIP12	0.98	Regulates cell cycle progression	Brunet et al., 2020
Appears only in co-treatment of methomyl and 10 µg/mL YWE group				
R113A	RING finger protein 113A	0.57	Controls stability, trafficking and activity of proteins, cell proliferation and differentiation, apoptosis, immune regulation, signaling and mitochondrial dynamics	Nakamura, 2011

Table 3

The list of functional proteins expressed by the protective effect of Yanang water extract (YWE). The relative quantitation of each sample is presented as log2.

Gene name	Matched protein	t-Test (p)	Log2 expression value				Function	Reference
			Methomyl	Methomyl + YWE (µg/mL)				
				2.5	5	10		
DIDO1	Death-inducer obliterator 1	0.04	7.79 ± 0.55	7.62 ± 0.46	–	–	Pro-apoptotic protein and is induced by apoptosis	Guerfali et al., 2008; Kumar et al., 2013
CUL5	Cullin-5	0.14	7.92 ± 1.60	8.71 ± 1.87	6.03 ± 0.18	–	Inhibits cell growth through ubiquitylating and degrading adenosine 3',5'-monophosphate-responsive element binding protein 1 (CREB1)	Chen et al., 2023

Table 4

The list of the differentially expressed functional proteins that share common datasets across all treatment groups. The relative quantitation of each sample is presented as log2.

Gene name	Matched protein	t-Test (p)	Log2 expression value					Function	Reference
			Untreated	Methomyl	Methomyl + YWE (µg/mL)				
					2.5	5	10		
MCM5	DNA replication licensing factor MCM5	0.67	8.10 ± 0.27	7.74 ± 0.21	8.21 ± 0.11	8.18 ± 0.14	8.08 ± 0.13	Improves growth and survival via inactivation of p53	Agarwal et al., 2007
CCNB2	G2/mitotic-specific cyclin-B2	0.44	8.69 ± 0.33	8.83 ± 0.08	8.98 ± 0.33	9.19 ± 0.11	9.01 ± 0.39	Positively regulates cell proliferation	Wu et al., 2021
IQGA1	Ras GTPase-activating-like protein IQGAP1	0.12	8.93 ± 0.33	7.37 ± 1.08	8.97 ± 0.02	8.09 ± 0.19	8.79 ± 0.10	Promotes cell proliferation and cell cycle progression, inhibits apoptosis	Sato et al., 2010; Zeng et al., 2018
RBBP6	Retinoblastoma-binding protein 6	0.01	8.45 ± 0.46	7.16 ± 0.38	7.92 ± 0.33	7.27 ± 0.06	8.20 ± 0.08	Promotes cell proliferation and inhibits apoptosis via p53 degradation	Motadi et al., 2011
JAK2	Tyrosine-protein kinase JAK2	0.77	5.22 ± 0.05	4.26 ± 0.35	4.42 ± 0.36	5.48 ± 1.76	5.07 ± 0.48	Enhances cell growth and survival	Kovanen et al., 2000
STOX2	Storkhead-box protein 2	0.19	9.98 ± 2.25	9.59 ± 2.10	9.42 ± 0.01	10.10 ± 0.11	9.73 ± 1.49	Suppresses apoptosis and promotes growth	Sasahira et al., 2016
PAWR	PRKC apoptosis WT1 regulator protein	0.99	4.77 ± 0.32	5.26 ± 0.84	6.01 ± 0.40	5.82 ± 0.05	4.99 ± 0.37	Promotes apoptosis	Shukla et al., 2016

Homeobox protein DLX-6 (DLX6), Spectrin alpha chain (SPTA1) and E3 ubiquitin-protein ligase TRIP12 (TRIPC) at a dose of 5 µg/mL, and RING finger protein 113A (R113A) at a dose of 10 µg/mL.

Moreover, 39 proteins were differentially expressed across the groups of methomyl treatment, and co-treatments of methomyl with YWE were also evaluated (Table S2). Of these, the expression levels of 2 apoptosis-related proteins, Death-inducer obliterator 1 (DIDO1) and Cullin-5 (CUL5) were found to have a marked decrease in a dose-dependent manner of YWE (Table 3).

Among the 423 proteins commonly identified in all 5 conditions (Table S3), 7 proteins are involved in apoptosis and cell cycle arrest. These include DNA replication licensing factor MCM5 (MCM5), G2/mitotic-specific cyclin-B2 (CCNB2), Ras GTPase-activating-like protein IQGAP1 (IQGA1), Retinoblastoma-binding protein 6 (RBBP6), Tyrosine-protein kinase JAK2 (JAK2), Storkhead-box protein 2 (STOX2), and PRKC apoptosis WT1 regulator protein (PAWR). Their expression levels exhibited slight changes, as shown in Table 4.

4. Discussion

Methomyl induces ROS formation, leading to oxidative stress (Jang et al., 2015), which can result in cell cycle arrest, apoptosis, or necrosis (He et al., 2022). Our findings consistently demonstrate methomyl induced apoptosis and cell cycle arrest in RAW 264.7 cells, as shown by AO/EB double staining and flow cytometry. However, supplementation with YWE significantly reduced these effects. One of the mechanisms in apoptosis induction involves the caspases. These enzymes are a conserved protein family activated after a cell receives pro-apoptotic signals (Heikal et al., 2014). Caspases associated with apoptosis have been classified into two groups based on their mechanisms: the initiator caspases, represented by caspase-9, and the effector caspases,

represented by caspase-3 (Shi, 2004). The literature indicates that exposure to methomyl, both caspase-9 and caspase-3, results in increased mRNA expression levels in experimental animals (Heikal et al., 2014; He et al., 2022). Our study confirms methomyl increases caspase-9 and -3 expression in RAW 264.7 cells, and YWE treatment reduces these levels.

Proteomic analysis suggests methomyl disrupts RAW 264.7 cell functions like apoptosis, cell cycle, and survival. RAW 264.7 cells exposed to methomyl displayed 4 unique proteins, which disappeared upon co-treatment with YWE. This suggests potential mitigation of methomyl cytotoxicity by YWE across all doses. RAC-alpha serine/threonine-protein kinase (AKT1) is a well-known protein kinase that plays a critical role in various vital biological processes, including cell survival, cell proliferation, and apoptosis (Hou et al., 2022). Gamma-aminobutyric acid receptor subunit alpha-3 (GBRA3), found exclusively in the methomyl treatment group, is a component of the Gamma-aminobutyric acid receptor (GABA). Despite its main function in the central nervous system, GABA has been linked to immune suppression, including promoting apoptosis and differentiation in T-helper cells (Meng et al., 2016). LAG1 longevity assurance homolog 1 (LASS1) and Programmed cell death protein 2-like (PDD2L or PD-2) functions are less known, but their family regulates apoptosis and proliferation. Yang et al. (2019) found LASS2 suppresses cell proliferation and induces apoptosis. LASS5 has been reported as a regulator in ceramide synthesis. An increase in ceramide has commonly been assumed to induce apoptosis and cell cycle arrest (Xu et al., 2005; Gomez-Larrauri et al., 2020). Similarly, the interaction of PD-1 with its ligand triggers lymphocyte deletion by downregulating proliferation and cytokine production (Bertsson et al., 2018). Meanwhile, PD-4 can initiate apoptosis by inhibiting protein translation (Lankat-Buttgereit and Goke, 2003). The data reported here appear to support the assumption that 2.5 – 10 µg/mL YWE shows a

protective effect against apoptosis and cell cycle arrest via down-regulation of these proteins.

On the other hand, anti-apoptotic proteins were observed to be exclusively expressed only in the co-treatment group with YWE and methomyl. The function of CUB and sushi domain-containing protein 1 (CSMD1) remains limited due to a lack of thorough investigation. One explanation of its function is tumor suppressive activity in human breast cancer cells (Blom, 2017). Hemeobox protein DLX-6 (DLX6) belongs to the DLX family in humans, which includes DLX-1, DLX-2, DLX-3, DLX-5, and DLX-7. Interestingly, DLX-2 has been reported to hold anti-necrotic activity and could promote cell proliferation (Lee et al., 2011). Spectrin alpha chain (SPTA1), is one of the caspase targets, as well as myosin and vimentin. Karanam et al. (2010) suggest that SPTA1 levels depend on specific regulation and may indicate caspase activity linked to the mitochondrial apoptotic pathway. This supports our finding that SPTA1 presence might suggest an anti-apoptotic effect. E3 ubiquitin-protein ligase TRIP12 (TRIPC) plays crucial roles in various vital biological processes, including cell cycle progression, DNA/chromatin repair, and cell differentiation. Inactivation of TRIPC leads to cell cycle arrest and apoptosis (Brunet et al., 2020). The last outstanding protein in this group is RING finger (RNF) protein 113A (R113A). Common functions of RNF protein impact many routes of cellular and physiological processes, including cell stability, integrity, trafficking, proliferation, differentiation, apoptosis, signaling, and mitochondrial dynamics (Nakamura, 2011). The evidence from this study suggests that YWE dose influences protein expression through different cellular mechanisms. Notably, the higher dose appeared to have a significantly greater impact on inhibiting apoptosis and cell cycle arrest, while also inducing cell cycle progression.

Death-inducer obliterator 1 (DIDO1) and Cullin-5 (CUL5) were interestingly observed to be down-regulated in the co-treatment with YWE and methomyl. DIDO1, a pro-apoptotic protein, becomes overexpressed upon activation of the apoptotic signal, ultimately leading to cell death (Guerfali et al., 2008; Kumar et al., 2013). Meanwhile, CUL5 acts as a tumor suppressor. Its overexpression leads to inhibition of cell growth via ubiquitylating and degrading adenosine 3',5'-monophosphate-responsive element binding protein 1 (CREB1) (Chen et al., 2023). It is crucial to emphasize that suppression of these proteins was controlled in a dose-dependent manner by YWE. One possible implication of this is that the bioactive compound of YWE might be able to disrupt apoptotic signaling and promote cell cycle progression, by governing the critical functions of these proteins.

A total of 423 shared common datasets across 5 experimental groups were screened, of which 7 proteins were associated with apoptotic proteins. Among these 7 proteins, 6 proteins were up-regulated, and 1 protein was down-regulated. The first up-regulated protein was the DNA replication licensing factor MCM5 (MCM5). MCM5 is relevant to inactivation of p53 signaling, resulting in enhanced cell growth and survival (Agarwal et al., 2007). G2/mitotic-specific cyclin-B2 (CCNB2) is one of the most important proteins involved in cell cycle regulation. Its defect leads to the failure of the G2/M checkpoint during the cell cycle progression (Wu et al., 2021). Ras GTPase-activating-like protein IQGAP1 (IQGA1) is upregulated in breast cancer and promotes cell proliferation while regulating the cell cycle and suppressing apoptosis (Sato et al., 2010; Zeng et al., 2018). Retinoblastoma-binding protein 6 (RBBP6) interacts with p53 and pRb proteins, promoting cell proliferation by facilitating p53 protein degradation through its RNF domain (Motadi et al., 2011). Meanwhile, Tyrosine-protein kinase JAK2 (JAK2) and Storkhead-box protein 2 (STOX2) were similarly reported to promote cell growth, cell survival, and prevent apoptosis (Kovanen et al., 2000; Sasahira et al., 2016). In contrast, PRK apoptosis WT1 regulator protein (PAWR or Par-4) was observed to be down-regulated in YWE supplemented groups. Par-4 is one of the most well-known pro-apoptotic proteins and was identified in cancer cells. Secretion of Par-4 promotes apoptosis in cancer cells with specific activation through cell surface receptor GRP78 (Shukla et al., 2016). Moreover, their expression levels

were gradually agreeable with doses of YWE. Taken together, the observed up- and down-regulation of proteins by YWE suggests its potential to mitigate methomyl-induced toxicity, possibly by interfering with apoptotic and cell cycle pathways.

5. Conclusions

YWE protects RAW 264.7 cells from methomyl toxicity by reducing apoptosis and cell cycle arrest via suppressing caspase-9 and caspase-3 mRNA expression. Proteomic analysis reveals methomyl induces proteins associated with immune suppression and cell cycle arrest. Co-treatment with YWE and methomyl upregulates anti-apoptotic and cell cycle progression proteins, while suppressing pro-apoptotic proteins. This suggests that YWE disrupts apoptotic signaling and promotes cell cycle progression, preventing methomyl-induced cytotoxicity.

CRedit authorship contribution statement

Boonyarit Kukaew: Writing – original draft, Visualization, Investigation, Formal analysis. **Wanna Sirisangtragul:** Writing – original draft, Supervision, Methodology. **Sittiruk Roytrakul:** Writing – review & editing, Methodology, Investigation, Formal analysis. **Anupong Joompang:** Writing – original draft, Formal analysis. **Napaporn Roamcharern:** Writing – original draft, Validation, Formal analysis. **Anupong Tankrathok:** Writing – review & editing, Formal analysis. **Patralak Songserm:** Writing – original draft, Visualization. **Sakda Daduang:** Writing – review & editing, Supervision. **Sompong Klaynongsruang:** Supervision, Funding acquisition. **Nisachon Jangpromma:** Writing – review & editing, Visualization, Supervision, Methodology, Investigation, Funding acquisition.

Declaration of competing interest

The authors declare that they have no known competing financial interests or personal relationships that could have appeared to influence the work reported in this paper.

Acknowledgements

This work was supported by the Fundamental Fund of Khon Kaen University, the National Science, Research and Innovation Fund (NSRF), Thailand, and the Protein and Proteomics Research Center for Commercial and Industrial Purposes (ProCCI), Faculty of Science, Khon Kaen University, Thailand.

Appendix A. Supplementary material

Supplementary data to this article can be found online at <https://doi.org/10.1016/j.jksus.2024.103229>.

References

- Agarwal, M.K., Ruhl Amin, A.R., Agarwal, M.L., 2007. DNA replication licensing factor minichromosome maintenance deficient 5 rescues p53-mediated growth arrest. *Cancer Res.* 67 (1), 116–121.
- Berntsson, J., Eberhard, J., Nodin, B., et al., 2018. Expression of programmed cell death protein 1 (PD-1) and its ligand PD-L1 in colorectal cancer: Relationship with sidedness and prognosis. *Oncoimmunology* 7 (8), e1465165.
- Blom, A.M., 2017. The role of complement inhibitors beyond controlling inflammation. *J. Intern. Med.* 282 (2), 116–128.
- Bradford, M.M., 1976. A rapid and sensitive method for the quantitation of microgram quantities of protein utilizing the principle of protein-dye binding. *Anal. Biochem.* 72, 248–254.
- Brunet, M., Vargas, C., Larrieu, D., et al., 2020. E3 Ubiquitin Ligase TRIP12: Regulation, structure, and physiopathological functions. *Int. J. Mol. Sci.* 21 (22), 8515.
- Chen, S., Shao, F., Zeng, J., et al., 2023. Cullin-5 deficiency orchestrates the tumor microenvironment to promote mammary tumor development through CREB1-CCL2 signaling. *Sci. Adv.* 9 (3), eabq1395.
- Gomez-Larrauri, A., Presa, N., Dominguez-Herrera, A., et al., 2020. Role of bioactive sphingolipids in physiology and pathology. *Essays Biochem.* 64 (3), 579–589.

- Guerfali, F.Z., Laouini, D., Guizani-Tabbane, L., et al., 2008. Simultaneous gene expression profiling in human macrophages infected with *Leishmania major* parasites using SAGE. *BMC Genom.* 9, 238.
- He, D., Han, G., Zhang, X., et al., 2022. Oxidative stress induced by methomyl exposure reduces the quality of early embryo development in mice. *Zygote* 30 (1), 57–64.
- Heikal, T.M., Mossa, A.-T.-H., Khalil, W.K., 2014. Protective effects of vitamin C against methomyl-induced injuries on the testicular antioxidant status and apoptosis-related gene expression in rat. *J. Environ. Anal. Toxicol.* 5 (2), 1–7.
- Hou, L., Qiao, X., Li, Y., et al., 2022. A RAC- α serine/threonine-protein kinase (CgAKT1) involved in the synthesis of CgIFNLP in oyster *Crassostrea gigas*. *Fish. Shellfish. Immunol.* 127, 129–139.
- Jang, Y.J., Won, J.H., Back, M.J., et al., 2015. Paraquat induces apoptosis through a mitochondria-dependent pathway in RAW264.7 cells. *Biomol. Ther. (Seoul)* 23 (5), 407–413.
- Karanam, N.K., Grabarczyk, P., Hammer, E., et al., 2010. Proteome analysis reveals new mechanisms of Bcl11b-loss driven apoptosis. *J. Proteome Res.* 9 (8), 3799–3811.
- Kovanen, P.E., Junttila, I., Takaluoma, K., et al., 2000. Regulation of Jak2 tyrosine kinase by protein kinase C during macrophage differentiation of IL-3-dependent myeloid progenitor cells. *Blood* 95 (5), 1626–1632.
- Kumar, S., Nigam, A., Priya, S., et al., 2013. Lipoic acid prevents Cr(6+) induced cell transformation and the associated genomic dysregulation. *Environ. Toxicol. Pharmacol.* 36 (1), 182–193.
- Lankat-Buttgereit, B., Goke, R., 2003. Programmed cell death protein 4 (pdc4): A novel target for antineoplastic therapy? *Biol. Cell* 95 (8), 515–519.
- Lee, S.Y., Jeon, H.M., Kim, C.H., et al., 2011. Homeobox gene *Dlx-2* is implicated in metabolic stress-induced necrosis. *Mol. Cancer* 10, 113.
- Meng, J., Xin, X., Liu, Z., et al., 2016. Propofol inhibits T-helper cell type-2 differentiation by inducing apoptosis via activating gamma-aminobutyric acid receptor. *J. Surg. Res.* 206 (2), 442–450.
- Motadi, L.R., Bhoola, K.D., Dlamini, Z., 2011. Expression and function of retinoblastoma binding protein 6 (RBBP6) in human lung cancer. *Immunobiology* 216 (10), 1065–1073.
- Nakamura, N., 2011. The role of the transmembrane RING finger proteins in cellular and organelle function. *Membranes (Basel)* 1 (4), 354–393.
- Nazimek, K., Ptak, W., Marcinkiewicz, J., Bryniarski, K., 2013. Macrophage function in allergic and autoimmune responses. *J. Phys. Ther. Health Promot.* 1 (1), 36–45.
- Phunchago, N., Wattanathorn, J., Chaisiwamongkol, K., 2015. *Tiliacora triandra*, an anti-intoxication plant, improves memory impairment, neurodegeneration, cholinergic function, and oxidative stress in hippocampus of ethanol dependence rats. *Oxid. Med. Cell. Longev.* 2015, 918426.
- Sapbamrer, R., Kitro, A., Panumasvivat, J., et al., 2023. Important role of the government in reducing pesticide use and risk sustainably in Thailand: Current situation and recommendations. *Front. Public Health* 11, 1141142.
- Sasahira, T., Nishiguchi, Y., Fujiwara, R., et al., 2016. Storkhead box 2 and melanoma inhibitory activity promote oral squamous cell carcinoma progression. *Oncotarget* 7 (18), 26751–26764.
- Sato, A., Naito, T., Hiramoto, A., et al., 2010. Association of RNase L with a Ras GTPase-activating-like protein IQGAP1 in mediating the apoptosis of a human cancer cell-line. *FEBS J.* 277 (21), 4464–4473.
- Shi, Y., 2004. Caspase activation, inhibition, and reactivation: A mechanistic view. *Protein Sci.* 13 (8), 1979–1987.
- Shukla, N., Zhao, Y., Rangnekar, V., 2016. PAWR (PRKC apoptosis WT1 regulator protein; Prostate apoptosis response-4, Par-4), Atlas Genet Cytogenet Oncol Haematol.
- Singthong, J., Ningsanond, S., Cui, S.W., 2009. Extraction and physicochemical characterisation of polysaccharide gum from Yanang (*Tiliacora triandra*) leaves. *Food Chem.* 114 (4), 1301–1307.
- Singthong, J., Oonsivilai, R., Onmetta-Aree, J., et al., 2014. Bioactive compounds and encapsulation of Yanang (*Tiliacora triandra*) leaves. *Afr. J. Tradit. Complement. Altern. Med.* 11 (3), 76–84.
- Thong-Asa, W., Tumkiratwong, P., Bullangpoti, V., et al., 2017. *Tiliacora triandra* (Colebr.) Diels leaf extract enhances spatial learning and learning flexibility, and prevents dentate gyrus neuronal damage induced by cerebral ischemia/reperfusion injury in mice. *Avicenna. J. Phytomed.* 7 (5), 389–400.
- Trachantong, W., Saenphet, S., Saenphet, K., et al., 2017. Lethal and sublethal effects of a methomyl-based insecticide in *Hoplobatrachus rugulosus*. *J. Toxicol. Pathol.* 30 (1), 15–24.
- Tudi, M., Daniel Ruan, H., Wang, L., et al., 2021. Agriculture development, pesticide application and its impact on the environment. *Int. J. Environ. Res. Public Health* 18 (3), 1112.
- Wu, S., Su, R., Jia, H., 2021. Cyclin B2 (CCNB2) stimulates the proliferation of triple-negative breast cancer (TNBC) cells *in vitro* and *in vivo*. *Dis. Markers* 2021, 5511041.
- Xu, Z., Zhou, J., McCoy, D.M., et al., 2005. LASS5 is the predominant ceramide synthase isoform involved in de novo sphingolipid synthesis in lung epithelia. *J. Lipid Res.* 46 (6), 1229–1238.
- Yang, Y., Yang, X., Li, L., et al., 2019. LASS2 inhibits proliferation and induces apoptosis in HepG2 cells by affecting mitochondrial dynamics, the cell cycle and the nuclear factor-kappaB pathways. *Oncol. Rep.* 41 (5), 3005–3014.
- Zeng, F., Jiang, W., Zhao, W., et al., 2018. Ras GTPase-activating-like protein IQGAP1 (IQGAP1) promotes breast cancer proliferation and invasion and correlates with poor clinical outcomes. *Med. Sci. Monit.* 24, 3315–3323.